I&EC research
Industrial & Engineering Chemistry Research

Article

pubs.acs.org/IECR

Heat Transfer Characteristics of Alumina Membrane Coated Activated Carbon with Core−Shell Structure

Fengqiu Chen,[†,‡] Chenchen Cai,[‡] Dang-guo Cheng,*[,‡] and Xiaoli Zhan[‡]

[†]Key Laboratory of Biomass Chemical Engineering of Ministry of Education, Department of Chemical and Biological Engineering, Zhejiang University, Hangzhou 310027, China

[‡]Department of Chemical and Biological Engineering, Zhejiang University, Hangzhou 310027, China

ABSTRACT: Alumina membrane coated activated carbon particles with core−shell structure have been synthesized by a spraying process with different layer thicknesses. The effective thermal conductivity of particle bed was determined by the hot-wire method, and the particle thermal conductivity was calculated using the model of effective thermal conductivity in fixed-bed. The results indicate the particle thermal conductivity decreases with an increase in the coatings of alumina. In addition, the decreasing tendency is greater in core−shell structure than that in physical mixed cases. A heat transfer model is developed to deduce the particle thermal conductivity of materials with core−shell structure, which agrees well with the experimental data. The expression is $\lambda_p = 0.51v_s\lambda_s + 1/(2.03v_s/\lambda_s + 1.02v_c/\lambda_c)$. The developed model in this paper provides a method for studying heat transfer properties and predicting the particle thermal conductivity of the materials with core−shell structure.

1. INTRODUCTION

Recently, the preparation and application of core−shell structured catalysts, which usually comprise an inorganic membrane (shell) surrounding a solid particle (core), have attracted much attention due to their reaction space confinement and synergistic function.[1−4] Yang et al.[5] have synthesized H-ZSM-5/Co/SiO_2 catalysts with core−shell structure by a direct hydrothermal synthesis method and investigated their performance in Fischer−Tropsch synthesis. They have found that the FT-active site in the core can convert syngas into linear hydrocarbons, and then, the hydrocarbons move to the acidic sites of zeolite in which they undergo further hydrocracking and isomerization to form branched hydrocarbons. Due to the core−shell structure of catalyst, a one-step production of isoparaffin from syngas can be realized. Nishiyama et al.[6] have coated the SiO_2−Al_2O_3 catalyst particles by silicate-1 zeolite membranes for the disproportionation of toluene. They have found that the fraction of *p*-xylene in xylene isomers (*para*-selectivity) over the core−shell catalyst largely exceeded the equilibrium value of about 22%, which resulted from the selective removal of the produced *p*-xylene.

In addition, the shell can protect the core (or active site on it) and improve the stability of the catalyst. Tang et al.[7] have synthesized zeolite-encapsulated noble metal catalysts and found the zeolitic shell can prevent the large reactant and poison molecules from contacting the noble metal nanoparticles, which led to their good reactant selectivity and poison resistance. On the other hand, the shell prevented the encapsulated noble metal nanoparticles from leaching out of the zeolitic shell, ensuring high reusability of the catalysts. Previously, our group has synthesized alumina membrane coated activated carbon particles with core−shell structure aiming at the enhancement of its mechanical strength in chemical reactor. The shell (membrane) can protect AC and the attrition of activated carbon decreased from 12.6% to 2.9%. This offers a novel way to enhance the mechanical properties of solid catalyst.[8] It has also been proved that the coatings of alumina membrane have little effect on the microstructure of activated carbon. Subsequently, we employed the prepared material in CO hydrogenation and found that the heat transfer characteristics of the particles are certainly influenced by Al_2O_3 membrane outside because of the difference of thermal conductivity between Al_2O_3 and AC. It is necessary to study the heat transfer characteristics of the composite catalyst with core−shell structure. To the best of our knowledge, there is no relative work reported.

Thus, in this work, a series of alumina membrane coated activated carbon particles with different layer thicknesses will be synthesized by the spray-casting method. The effect of the layer thickness on the heat transfer properties of the materials will be investigated. On this basis, a model, which displays the relationship between the thermal conductivity of core−shell structured catalysts and the volume fraction of shell and core, will be developed finally.

2. EXPERIMENTAL SECTION

2.1. Sample Preparation. Activated carbon (AC) particles were coconut-shell based (particle size: 450−900 μm, Sichuan Lvyuan Co., China). Alumina membrane coated activated carbon (AC@Alumina) samples were prepared by the sol−gel spray-casting method. Boehmite sol was prepared by the Yoldas process[9] using aluminum isopropoxide as the precursor. Briefly, aluminum isopropoxide was first hydrolyzed in water at 80 °C and stirred for 1 h. Then nitric acid (1.45 mol·L^{-1}) was added, and the sol was refluxed for 12 h at 90 °C, followed by exposure to air at 90 °C for 2 h. The resulting boehmite sol (solid concentration is about 7%) was diluted in ethanol (sol/ethanol

Received: July 31, 2012
Revised: February 13, 2013
Accepted: February 14, 2013
Published: February 14, 2013

= 1:6−1:9). Thereafter, the sol was sprayed on AC particles uniformly and dried at 120 °C for 1 h. The spray−dry process was repeated for more than 10 times. Finally, the prepared particles were calcined at 500 °C for 4 h in N_2 atmosphere. The thickness of the alumina membranes on AC particles can be controlled by the times of spraying and the concentrations of boehmite sol. Four samples with different layer thicknesses, marked as CS1, CS2, CS3, and CS4, were synthesized. The alumina volume fraction is 0.0169, 0.0369, 0.0815, and 0.105, respectively. In addition, for comparison, another series of samples (MX1, MX2, MX3, and MX4) with the same alumina content were prepared by simple mixing of AC and γ-alumina (particle size: 75 to 175 μm, Sinapharm Chemical Reagent Co., China) in a beaker through stirring for more than 30 min until the particles were mixed uniformly.

2.2. Characterization. X-ray diffraction (XRD) patterns were collected on an X-ray diffractometer (Shimadzw, XRD-6000) equipped with Cu Kα radiation at a working voltage of 40 kV and a current of 40 mA. The morphology of the samples was examined by a scanning electron microscope (SEM, Hitachi TM-1000).

2.3. Thermal Conductivity Measurement. The thermal conductivity of the prepared particles was measured by the hot-wire method.[10] This method is based on the measurement of temperature increase with respect to time at a specified distance from the wire. In this work, the thermal conductivity and the electric resistance of the wire were deemed to be constants because the particles were measured in a short temperature range (20−50 °C). The sample container was a stainless-steel box (40 × 40 × 95 mm). The wire (R = 1.7 Ω) was through the middle line of the box and mixed at both sides. A chrome-nickel wire with a diameter of 0.4 mm and a length of 95 mm was used for the hot wire, and it served as both a heating unit and an electrical resistance thermometer. Initially, the wire was kept at equilibrium with a full container of particles bed surrounding. Then, a regulation voltage (U = 0.95−1.50 V) was introduced to initiate the measurement. The thermal conductivity was calculated from the slope of the rise in the wire's temperature against the logarithmic time interval. By employing a K-type thermocouple to monitor the temperature of the particles near the wire, within the special time intervals, a linear relationship ($t = k \ln \tau + a$) can be acquired. Finally, the effective thermal conductivity of the particles can be determined by eq 1:[10]

$$\lambda_e = \frac{dt}{d \ln \tau} \times \frac{P}{4\pi} = \frac{kP}{4\pi} \quad (1)$$

where λ_e is the effective thermal conductivity ($W \cdot m^{-1} \cdot °C^{-1}$), P is the power per unit length of hot-wire ($W \cdot m^{-1}$), τ is the time from starting heating to recording, and t is the temperature at recording time.

3. RESULTS AND DISCUSSION

3.1. Characterization. A series of AC@Alumina particles (CS1, CS2, CS3, CS4) were prepared by a spraying process with different layer thicknesses. The relative properties are listed in Table 1. The XRD patterns of the represented samples are shown in Figure 1. Besides the characteristic peaks of AC, the one located at 67.0° can be assigned to that of γ-Al_2O_3.[11]

Overall SEM image of AC@Alumina samples is shown in Figure 2. It is evident that AC particles are completely coated with a homogeneous alumina membrane. Cross-sectional SEM images of AC@Alumina samples are shown in Figure 3, which indicates that the dense alumina membrane is combined compactly with AC particle, and the layer thickness of four samples is 2.1, 4.1, 7.4, and 12.3 μm, respectively.

Table 1. Properties of the Core−Shell Structured Samples

sample	ρ/g·mL^{-1} (density)	ω_s/% (mass fraction)	υ_s/% (volume fraction)	d/μm (thickness of membrane)
AC	1.20	0	0	0
CS1		2.17	1.69	2.1
CS2		4.71	3.69	4.1
CS3		10.29	8.15	7.4
CS4		13.11	10.46	12.3
Al_2O_3	1.55	100	100	

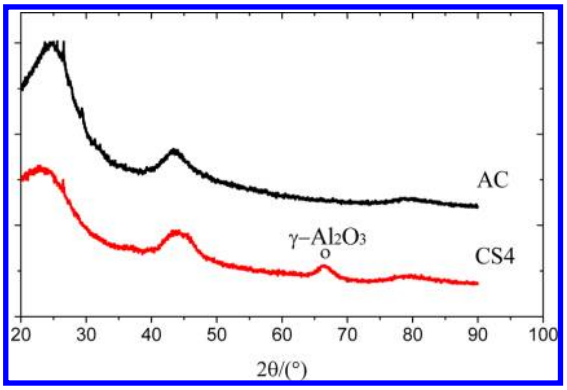

Figure 1. XRD patterns of AC and CS4 particles.

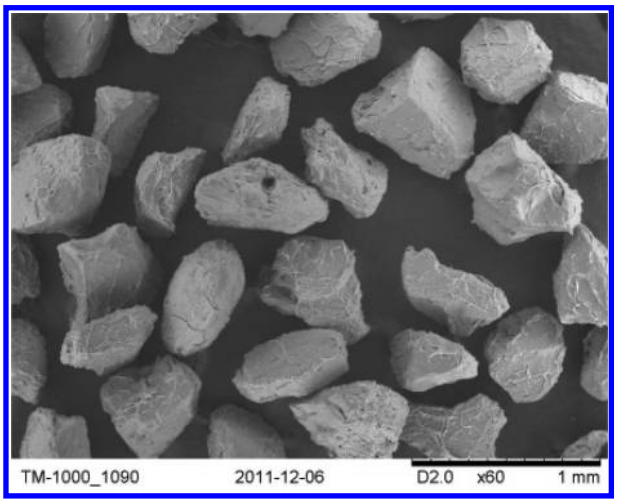

Figure 2. Overall SEM images of AC@Alumina particles.

The N_2 adsorption tests indicate that BET surface area of AC and AC@Alumina is 810.0 and 727.7 m^2/g, respectively,[8] and activated carbon contributes to the micropore of the sample of AC@Alumina. The coatings of the alumina membrane do not affect the microstructure of activated carbon.

3.2. Determination of Thermal Conductivities. Compared with AC particles, the heat transfer properties of AC@Alumina particles are certainly influenced by the alumina membrane due to the difference of thermal conductivities between alumina and AC. On the other hand, the contact media of the particles should be alumina when used in the chemical reactor, which also affects the thermal conductivities.

The effective thermal conductivities of the particles (λ_e) determined by the hot-wire method are listed in Table 2. The results show that the effective thermal conductivity of alumina is much smaller than that of AC, and the effective thermal

dx.doi.org/10.1021/ie303318t | Ind. Eng. Chem. Res. 2013, 52, 3653−3657

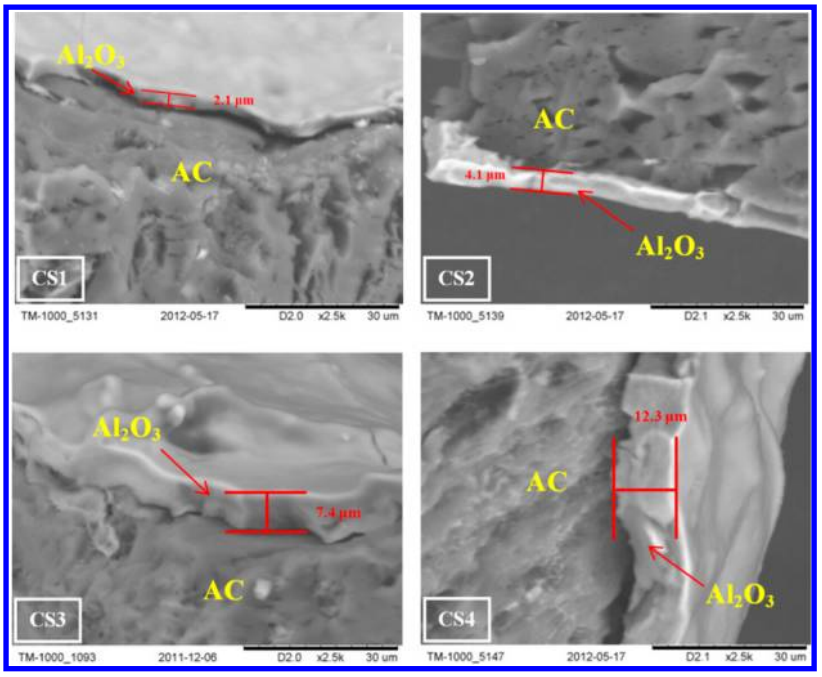

Figure 3. Cross-sectional SEM images of AC@Alumina particles.

Table 2. Effective Thermal Conductivities of the Samples

sample	ε/% (bed voidage)	P/W·m^{-1} (power)	k ($dt/dln\tau$)	λ_e/W·m^{-1}·°C^{-1} (effective thermal conductivity)
AC	40	7.08	2.75	0.205
CS1	40	7.08	2.89	0.195
CS2	40	7.62	3.21	0.189
CS3	40	8.14	3.58	0.181
CS4	40	8.25	3.75	0.175
Al_2O_3	38	7.97	4.53	0.140

conductivity of AC@Alumina particles decreases with increasing coating alumina.

In order to study on the heat transfer characteristics of AC@Alumina particles more directly, it is necessary to determine the particle thermal conductivity (λ_p). According to previous research,[12,13] there is a relationship between the effective thermal conductivity (λ_e) and the thermal conductivity of fluid (λ_f) by ignoring the influence of radiation in a static system, which is shown in eq 2:

$$\lambda_e/\lambda_f = \varepsilon + \frac{1-\varepsilon}{\phi + 2\lambda_f/3\lambda_p} \quad (2)$$

where λ_f represents thermal conductivity of fluid and ϕ represents the effect of the fluid film at the contact point of particles, which can be calculated by eq 3:

$$\phi = \phi_2 + (\phi_1 - \phi_2)(\varepsilon - 0.26)/0.216 \quad (3)$$

The value of ϕ_1 and ϕ_2 are in relation to the ratio of particle thermal conductivities to fluid thermal conductivities and determined by fitting the curves given in the previous research.[12,13] The particle thermal conductivities are calculated with eq 2, and the results are shown in Figure 4. It can be seen that the changes tendency of particle thermal conductivity is similar to that of effective thermal conductivity.

In addition, to investigate the effects of core−shell structure on the thermal conductivities of particles, AC particles were mixed physically with alumina particles (MX1, MX2, MX3, MX4) in the same composition ratio with AC@Alumina samples. Their calculated particle thermal conductivities are also included in Figure 4. One can see that the changes tendency of the curves is different. With increasing alumina content, the decreasing tendency of particle thermal conductivities is greater in core−shell structure than that in physical mixed cases. With the same composition ratios, the particle thermal conductivities of AC@Alumina samples are about 10−20% smaller than that of mixed samples.

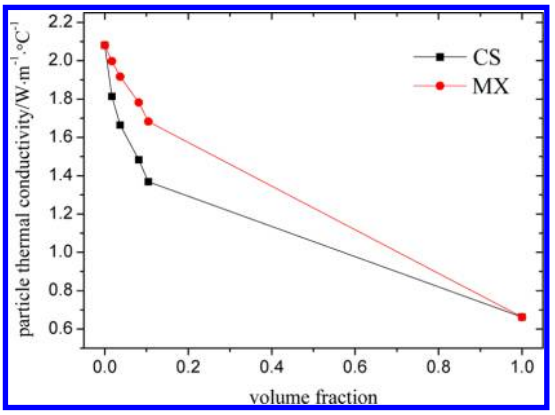

Figure 4. Comparison of particle thermal conductivities of the samples with core−shell structure and physically mixed.

3.3. Heat Transfer Model of the Particles with Core−Shell Structure. To study the thermal characteristics of composite materials with some complicated structure, the method of dividing the configuration of materials was used to build models.[14] According to the reported results, a heat transfer model of the core−shell structured particles is developed in this work.

In the model, shown in Figure 5, an AC@Alumina particle in an irregular shape is simplified into a cube and divided into two parts of thermal resistance unit in the heat flow direction: Al_2O_3-only unit and Al_2O_3-AC-Al_2O_3 composited unit. The Al_2O_3-AC-Al_2O_3 composited unit is surrounded by the Al_2O_3-

dx.doi.org/10.1021/ie303318t | Ind. Eng. Chem. Res. 2013, 52, 3653−3657

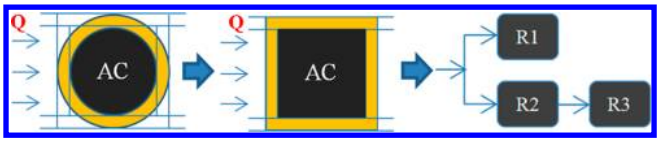

Figure 5. Heat transfer model of AC@Alumina particles.

only unit. On this assumption, the equivalent thermal resistance is diagramed in Figure 5, where R1 represents the thermal resistance of Al_2O_3-only unit and R2-R3 represents the thermal resistance in series of Al_2O_3-AC-Al_2O_3 composited unit, and the equivalent thermal resistances of the two units are arrayed in parallel in the heat flow direction. According to the computational method of series-parallel models,[15] the particle thermal conductivity can be calculated with a mathematical model as described in eq 4:

$$\lambda_p = av_s\lambda_s + \frac{1}{\frac{bv_s}{\lambda_s} + \frac{cv_c}{\lambda_c}} \quad (4)$$

where λ_s and λ_c represent the particle thermal conductivities of alumina and AC, respectively, v_s and v_c represent the volume fractions of alumina and AC, respectively, and a, b, and c are parameters.

The parameters are set to describe the impact of each heat transfer unit in the series-parallel model. The physical meaning and influencing factors of the parameters (a, b, and c) given in this model are discussed according to the relationship of thermal resistance and thermal conductivity ($R = l/(s\cdot\lambda)$). It can be analyzed easily that: parameter a represents the impact of the transfer length of the Al_2O_3-only unit in the heat flow direction and the ratio of alumina in two units, which is influenced mainly by the particle size; parameters b and c represent the impact of the transfer area of the Al_2O_3-AC-Al_2O_3 composited unit in the heat flow direction and the ratio of alumina in two units, which is influenced mainly by the particle size and the thickness of membrane.

The values of the parameters (a, b, and c) can be obtained by a regression analysis with eq 4 using the experimental data. Thus, the heat transfer model of the particles with core−shell structure that developed in this work is obtained with an expression as eq 5:

$$\lambda_p = 0.51v_s\lambda_s + \frac{1}{2.03v_s/\lambda_s + 1.02v_c/\lambda_c} \quad (5)$$

where the subscript s represents the shell and the c represents the core.

The comparison of calculated values of particle thermal conductivities with this model and with experimental data is shown in Figure 6. The correlation coefficient is 98.61%, and the average relative deviation is 2.04%, which indicates that this model expression agrees well with experimental data.

To validate our model, a new sample (CS5) has been prepared, which has the same structure with CS1-4 while the fraction of alumina is 0.0573. After using the experimental method to determine the effective thermal conductivity and particle thermal conductivity of CS5, the results are: λ_e = 0.184 $W\cdot m^{-1}\cdot°C^{-1}$, λ_p = 1.54 $W\cdot m^{-1}\cdot°C^{-1}$. Compared with the particle thermal conductivity (λ_p = 1.58 $W\cdot m^{-1}\cdot°C^{-1}$) that is calculated by the model with this new sample, the deviation is 2.53%. This indicates that our developed model is reliable and can predict the particle thermal conductivities of the materials with core−shell structure.

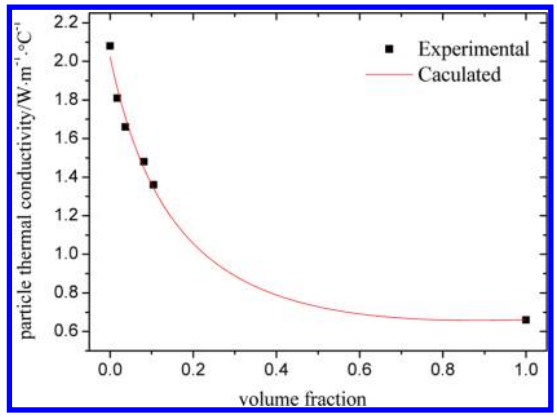

Figure 6. Comparison of experimental and calculated value of particle thermal conductivities of core−shell structured particles.

4. CONCLUSIONS

(1) Active carbon particles can be completely coated with a dense and homogeneous γ-alumina membrane by the spraying process, and the thickness of alumina membrane can be controlled from 2.1 to 12.3 μm by the number of times spraying and the concentrations of boehmite sol.

(2) The particle thermal conductivity decreases with the increase in the coating of alumina due to the weaker heat transfer capacity of alumina than that of active carbon. In addition, the particle thermal conductivities of particles with core−shell structure are about 10−20% smaller than that in physical mixed cases with the same weight composition ratios.

(3) A series-parallel heat transfer model of particles with core−shell structure is developed to describe the equivalent particle thermal conductivity, simplifying the influence of particle shape. A mathematical model is developed to match the relationship of particle thermal conductivity of particles with core−shell structure and the fraction of shell and core. The expression is $\lambda_p = 0.51v_s\lambda_s + 1/(2.03v_s/\lambda_s + 1.02v_c/\lambda_c)$, which agrees well with experimental data (R = 98.61%), and the parameters are influenced by the particle size and the thickness of the membrane. The developed model in this paper can reasonably predict the particle thermal conductivity of similar catalyst materials with core−shell structure.

AUTHOR INFORMATION

Corresponding Author

*Tel.: +86-571-8795-3382. E-mail: dgcheng@zju.edu.cn.

Author Contributions

All authors have given approval to the final version of the manuscript.

Notes

The authors declare no competing financial interest.

ACKNOWLEDGMENTS

Financial support from National Natural Science Foundation of China (21176211) and State Key Laboratory of Chemical Engineering of China (SKL-ChE-09D02) is gratefully acknowledged. The authors also thank Prof. Y.S. Lin at Arizona State University for his valuable discussion.

ABBREVIATIONS

λ_e = effective thermal conductivity of particle bed
λ_p = particle thermal conductivity
λ_f = thermal conductivity of fluid
λ_s = particle thermal conductivity of the material in shell
λ_c = particle thermal conductivity of the material in core
υ_s = volume fraction of shell
υ_c = volume fraction of core
P = power per unit length of the hot-wire
τ = time from starting heating to recording
t = temperature at recording time
k = parameter set to represent $(dt)/(d \ln \tau)$
ρ = density of particles
ω_s = mass fraction of alumina
d = thickness of alumina membrane
ε = bed voidage
ϕ = effect of the fluid film at the contact point of particles
ϕ_1, ϕ_2 = parameter set to calculate ϕ
U = direct voltage
R = electric resistance

REFERENCES

(1) Kamata, K.; Lu, Y.; Xia, Y. N. Synthesis and characterization of monodispersed core-shell spherical colloids with movable cores. *J. Am. Chem. Soc.* **2003**, *125*, 2384−2385.

(2) Khan, E. A.; Rajendran, A.; Lai, Z. Synthesis of Ni-SiO_2/silicalite-1 core-shell micromembrane reactors and their reaction/diffusion performance. *Ind. Eng. Chem. Res.* **2010**, *49*, 12423−12428.

(3) Jin, W.; Cheng, D.; Chen, F.; Zhan, X. Synthesis and application of zeolite membrane encapsulated catalysts. *Prog. Chem.* **2011**, *23*, 2021−2030.

(4) Kim, J.; Lee, J. E.; Lee, J.; Yu, J. H.; Kim, B. C.; An, K.; Hwang, Y.; Shin, C. H.; Park, J. G.; Hyeon, T. Magnetic fluorescent delivery vehicle using uniform mesoporous silica spheres embedded with monodisperse magnetic and semiconductor nanocrystals. *J. Am. Chem. Soc.* **2006**, *128*, 688−689.

(5) Yang, G.; He, J.; Yoshiharu, Y. Preparation, characterization and reaction performance of H-ZSM-5/cobalt/silica capsule catalysts with different sizes for direct synthesis of isoparaffins. *Appl. Catal., A* **2007**, *329*, 99−105.

(6) Nishiyama, N.; Miyamoto, M.; Egashira, Y. Zeolite membrane on catalyst particles for selective formation of p-xylene in the disproportionation of toluene. *Chem. Commun.* **2001**, *9*, 1746−1747.

(7) Ren, N.; Yang, Y.; Shen, J.; Zhang, Y.; Xu, H.; Gao, Zi.; Tang, Y. Novel, efficient hollow zeolitically microcapsulized noble metal catalysts. *J. Catal.* **2007**, *251*, 182−188.

(8) Chen, F. Q.; Hou, C. Y.; Cheng, D. G.; Zhan, X. L. A preparation method of activated carbon coated by alumina membrane. China patent, CN201010220428.9, 2010-11-24.

(9) Buelna, G.; Lin, Y. S. Sol-gel-derived mesoporous gamma-alumina granules. *Microporous Mesoporous Mater.* **1999**, *30*, 359−369.

(10) ISO 8894-1:1987. *Refractory materials-Determination of thermal conductivity-Part 1: Hot-wire method (cross-array) (MOD)*; ISO: Geneva.

(11) Shang, L.; Wang, Z.; Chuai, X.; Sun, B.; Wang, C.; Jiao, X. Preparation and identification of alumina in 8 crystal form. *Chem. World* **1994**, *7*, 346−350.

(12) Chen, G. *Chemical Reaction Engineering*; Chemical Industry Press: Beijing, 2007.

(13) Kunii, D.; Smith, J. M. Heat transfer characteristics of porous rocks. *AlChE J.* **1960**, *6*, 71−78.

(14) Agari, Y.; Uno, T. Estimation on thermal conductivities of filled polymers. *J. Appl. Polym. Sci.* **1986**, *32*, 5705−5712.

(15) Chen, Z.; Qian, J.; Ye, Y. Predicting theory of effective thermal conductivity of complex material. *J. Univ. Sci. Technol. Chin.* **1992**, *22*, 416−424.